*Original Research Article*

# Sandy Soil Compression Test Data to compute Compression Index

## Andrea Formato[1*] and Aurelio Liguori[2]

[1]Prof., Department of Agricultural Science. University of Naples "Federico II". Via Università 100, 80045, Portici, Naples, Italy.

[2]Prof., Univeristy "G. Fortunato". Viale Raffaele Delcogliano, 12, 82100 Benevento, Italy.E-mail: aurelio.liguori@fastwebnet.it

**\*Corresponding Author's E-mail: formato@unina.it
Tel./fax: +39812539150**

**Abstract**

**Through the hydrostatic compacting tests, it has been possible to evaluate the compression index Cc, that is the soil compaction index. Generally, the parameter Cc is affected by the soil granulometry composition and moisture content. In this paper, they have been examined 24 soil typologies representative of almost all types of sandy soils, to determine the compression index (Cc) denoting the soil compaction capability, and alterations in the Cc value when soil granulometry composition and moisture change. The soil samples were submitted to a hydrostatic compression test (HCT). Pressure-void index (p-e) diagrams were obtained, from which the compression index (Cc) was determined using the Gompertz model. The modulus of the slope of the virgin compression curves – the compression index (Cc) – were estimated as the modulus of the slope at the first inflection point of the Gompertz curve. The Gompertz model parameters were evaluated using a nonlinear regression method. The model fit the raw data closely, with mean R2 values greater than 0.99. The results reveal how the Cc index changes when the granulometry and humidity values change. Further, the experimental data 3D diagrams provide a better description of the mechanical behaviour of a family set of soils.**

**Keywords:** Gompertz model, hydrostatic soil compression test, sandy soil, soil compression index

## INTRODUCTION

When soils become compacted agricultural incomes are reduced, and the energy spent for the soil workmanship increase (Keller et al., 2007; Botta et al., 2008). Better workmanship tools can be obtained if the soil mechanical behaviour is known. Therefore, knowledge regarding the physical-mechanical properties of an agricultural soil can be used to forecast the reaction of the soil to mechanical action (Botta et al., 2006; Peruzzi et al., 2008). Thus, more suitable tools and machineries that better satisfy the specific requirements of the considered soil can be realized. Indeed, the soil-tool interaction phenomena must be considered, and it has previously been examined by many authors. (Chaney et al., 2001; Beylich et al., 2010). Further, it is necessary to evaluate the hydrostatic compression tests to determine the soil characteristics

(Formato et al. 2005; Karmakar and Kushwaha, 2006; Vallejos, 2008; Tekeste et al., 2009). The soil compression characteristic is a fundamental mechanical property of the soil that relates the effect of compressive stress on the soil volumetric parameter (Abo-Elnor et al., 2003; Formato, 2005; Mekkiyah and Al-Khazragie, 2015). Typically, the characteristic is illustrated by plotting the hydrostatic compression value *p* against soil void ratio *e*. The modulus of the slope of the compression curve is named the compression index (*Cc*).The *Cc index* represents the susceptibility of a soil to damage by compaction (Gregory et al., 2006; Güllü et al., 2016). Indeed, the compression diagrams can be related to the mechanical characteristics of agricultural soils. Methods to determine the soil compaction value, obtained after

application of a determined load have also been investigated by numerous authors by using complex models for the considered soil (Kumar et al., 2015). Here, the compression index *Cc* was determined via the compaction diagrams obtained by HCT of different soil samples using the Gompertz interpolation method.

## Curve Fitting and Compression Index Cc Estimate

The soil compression characteristic is a fundamental mechanical property that relates the effect of compressive or hydrostatic stress to a soil volumetric parameter. Typically, this characteristic is illustrated by plotting a logarithm (usually to base 10) of the compressive or hydrostatic stress against soil void ratio *e* (or other equivalent property). When expressed in this way, the characteristic has two distinct regions: an elastic rebound curve at low stress and a linear virgin compression curve – normally a consolidated path – at a higher stress. The modulus of the slope of the virgin compression curve is commonly called the compression index *Cc*. The transition point between the elastic rebound curve and the virgin compression curve is known as the soil pre-compression or pre-consolidation stress. In this paper, the Gompertz model has been used because of its ability to describe the compression phenomenon of a soil:

$$e = a + c \times E^{-E^{b(log_{10}p-m)}} \qquad (1)$$

Where *a, b, c* and *m* are fitting parameters, *e* is the soil void ratio, *p* is the compressive or hydrostatic effective stress, and *E* is the Euler number. The Gompertz function is routinely used to describe the reduction of a soil void ratio as well as the growth of its relative density, depending on the parameter *b*. This function is *S*-shaped, asymmetrical about the inflection point, and has two asymptotes: the first located at the initial soil void ratio ($e_{max} = a + c$) and the second at minimum ratio ($e_{min} = a$). The *Cc* was estimated as the modulus of the slope at the first inflection point ($Log_{10} p = m$) of the Gompertz curve: *m* is the abscissa of the point that marks the linear part of the curve itself. *Cc*, after some mathematical manipulation of the Gompertz function, can be generally expressed through the formula:

$$C_c = \frac{b \times c}{E} \qquad (2)$$

## MATERIALS AND METHODS

In this paper, soils with different typologies have been considered, with representation of almost all types of sandy soils. The soils were obtained considering three

soil granulometry types: type A(1- 0.5 mm), B(0.5-0.25 mm) and C(< 0.25 mm). Upon mixing of these three type types, 24 soil samples with granulometry content ranging from 0 to 100% in 20% increments were obtained. The soil samples are shown in Table 1. Further, different moisture contents of 0% (U0), 5% (U5) and 10% (U10) were considered. The soil sample specimens were prepared following the procedure illustrated in the report by Formato *et al.*, 2013. The samples were subsequently submitted to a Hydrostatic Compression Test (HCT).

The equipment shown in Figure 1 was used to perform the HCT.

## Test execution

The soil samples were submitted to HCT with a load cycle from 0to $1.5 \times 10^2$ kPain steps of 1 kPa. After each incremental step of 1kPa, the pressure was held constant for approximately 5 minutes. Despite the pressure remaining constant, the soil sample volumes continued to change. After 5 minutes, however, the changes in the soil sample volumes at the considered constant pressure value were almost negligible. These final volumes were recorded and reported in a (*p - e*) diagram.

Every test was performed 3 times. Statistical analyses were carried out using StatgraphicsPlus Package 4.1 STATPOINT TECHNOLOGIES, INC., (Warrenton, Virginia, USA). Variance and media analysis were calculated to determine the percent error for the considered tests.

To evaluate the Cc parameter, the results were fit using the Gompertz model. Although the *Cc* estimate based on the Gompertz inflection point has the advantage of being objectively defined by a straightforward procedure, this approach does have some drawbacks. First, the inflection point must lie within the range of the raw data; if not, any *Cc* estimate will be based on insufficient data to define the linear range and hence the slope. This is true for all numerical methods routinely employed, not just those based on the Gompertz model. Second, the lower asymptote *a* of the Gompertz model has significant statistical influence on the estimate of the *Cc*. Indeed, if the Gompertz model is an appropriate description of a soil compression process, then *a* should correspond to the water-filled void ratio $e_w$ or, if water was forced out of the voids, to zero *e* or some intermediate equilibrium value. Considering the sand as an aggregate of little spheres and if the latter have equal diameters, the minimum voids ratio will be equal to 0.33. This result is confirmed by observations in nature, where the void ratio of a sand ranges between 0.30 and 1. Therefore, constraining the fitted *a* parameter to this range is possible.

The estimates of the Gompertz model parameters and the statistical analysis reported in this paper were

**Table 1.** Soilgranulometry considered with weight  %, on dry soil

| Soil Type | Granulometry type A | Granulometry type B | Granulometry type C |
|---|---|---|---|
| S01 | 0 | 0 | 100 |
| S02 | 0 | 20 | 80 |
| S03 | 0 | 40 | 60 |
| S04 | 0 | 60 | 40 |
| S05 | 0 | 80 | 20 |
| S06 | 0 | 100 | 0 |
| S07 | 20 | 0 | 80 |
| S08 | 40 | 0 | 60 |
| S09 | 60 | 0 | 40 |
| S10 | 80 | 0 | 20 |
| S11 | 100 | 0 | 0 |
| S12 | 20 | 80 | 0 |
| S13 | 40 | 60 | 0 |
| S14 | 60 | 40 | 0 |
| S15 | 80 | 20 | 0 |
| S16 | 20 | 60 | 20 |
| S17 | 20 | 40 | 40 |
| S18 | 20 | 20 | 60 |
| S19 | 60 | 20 | 20 |
| S20 | 40 | 20 | 40 |
| S21 | 20 | 20 | 60 |
| S22 | 60 | 20 | 20 |
| S23 | 40 | 40 | 20 |
| S24 | 20 | 60 | 20 |
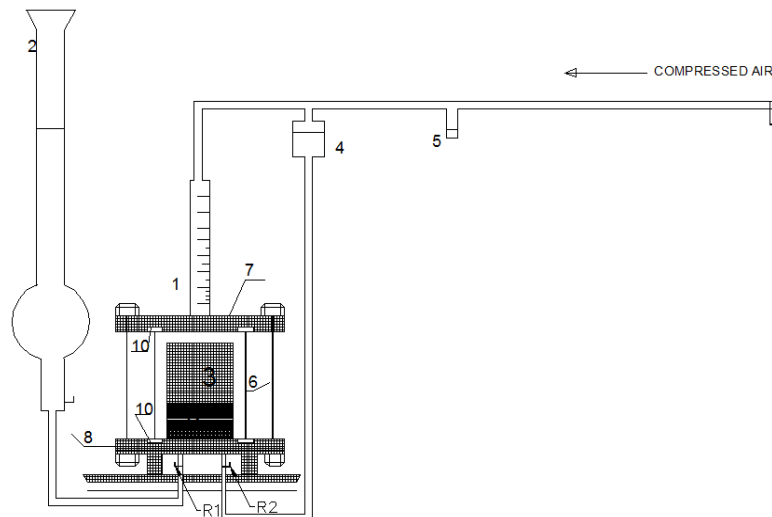


**Figure 1.** Equipment scheme to perform Hydrostatic Compression Test

1graduated burette to measure the total volume of the soil specimen;
2graduated burette with reference line;
3 soil specimen in the test cell;
4volumetric auxiliary capacity for the water recovery;
5 pressure transducer;
6clamping screws;
7top flange;
8bottom flange;
9 seat for the soil specimen;
10 sealed ring
R1 tap – open only during the volume measuring phase;
R2 tap – open only during the topping up phase;
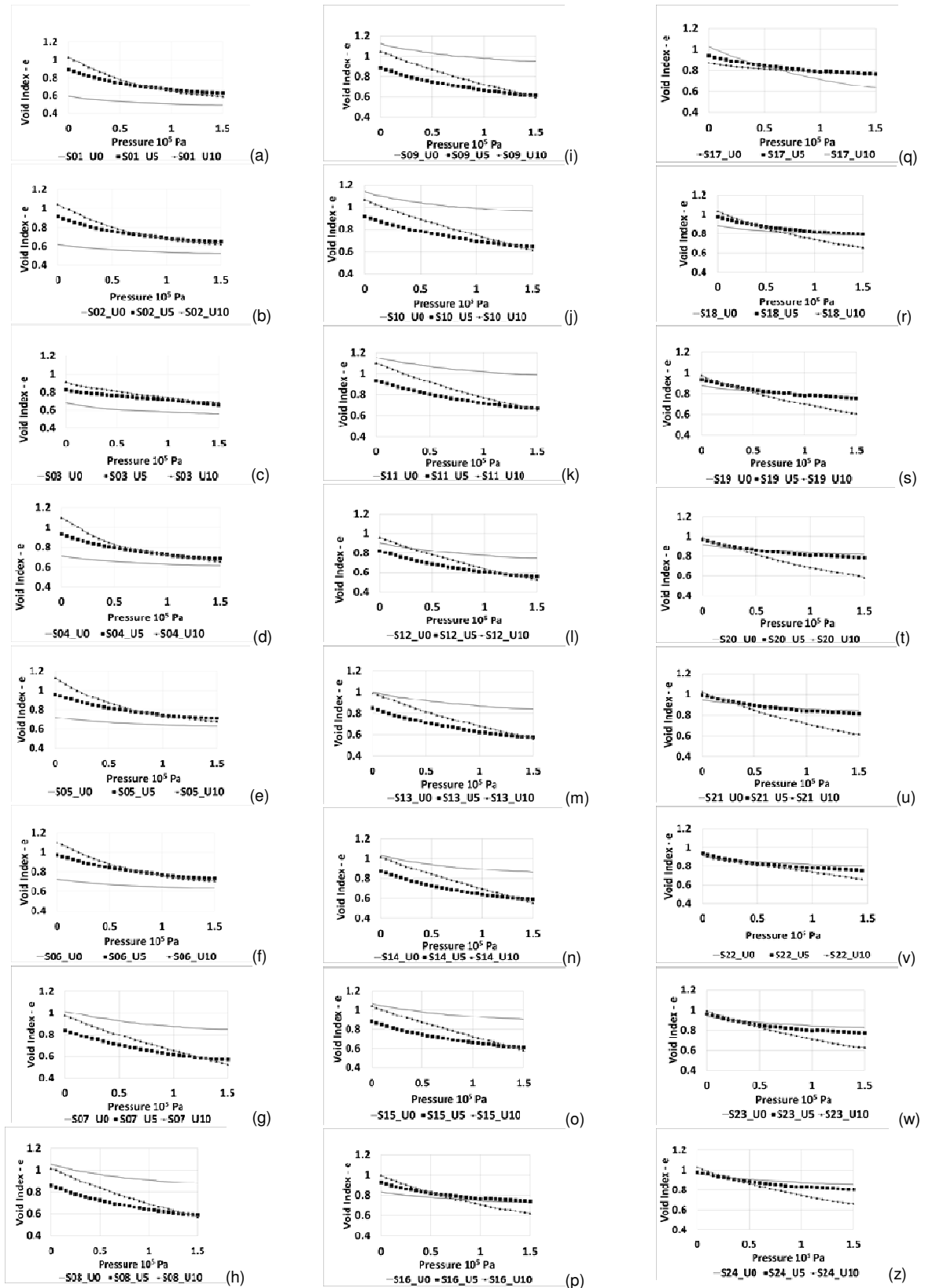
**Figure 2.** Diagrams p - e obtained by hydrostatic compression tests for the soil samples considered at moisture values of 0,5,10 % (U0, U5, U10).
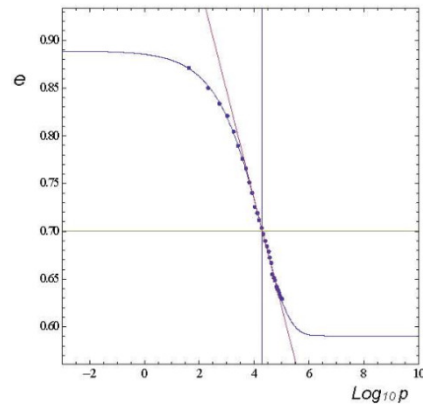
**Figure 3.** Raw data of the S01_U5 soil compression test, the fitting Gompertz model and the maximum slope line

performed using the Nonlinear Regression Package of Wolfram Mathematica 7 software.

**RESULTS**

In Figure 2, the $p - e$ diagrams for the soil samples with different moisture contents are shown (0, 5 and 10% in weight of water). The diagram points represent the mean value of the three tests performed. The maximum error detected for all the performed tests was less than 5%.

From the $p$-$e$ diagrams, a good correspondence to the well-known behaviour of soil submitted to compression tests can be seen. The curves obtained by the hydrostatic compression tests demonstrate that the unsaturated soil behaviouris quite similar to that of a saturated soil during the drained compression tests. Starting from an initial value of the voids ratio, the soil shows a decreasing value with increasing pressure. We have noted that these data results are in agreement with the results obtained by previous studies available in literature.

Three values of moisture content we reconsidered and we have noted that every curve shows a limit value, consolidation curve, and this is in agreement with the data results obtained by numerous authors. We can note that in the $p$-$e$ diagrams, the initial voids ratio increases when the moisture content increases, in agreement previous work (Ansorge and Godwin., 2009; Honda et al., 2011). Further in these diagrams, the curve slope increases when the big granulometry A increases in the soil composition and decreases when the moisture content increases. This behaviour is in agreement with the findings of numerous authors (Mosaddeghi et al., 2007; Singh., 2012; Tiwari and Ajmera, 2012). That is, the soils become more sensible to the effects of the compression loads when the big granulometry A increases. When the moisture content increases, this

effect decreases. Finally, the Gompertz model was used to evaluate the Cc for each soil. In the findings of numerous authors, it has been found that the Gompertz function and its associated estimations of Cc appeared to be the most appropriate. In fact it has been found that the Gompertz function effectively modelled compression data for tests on intact soil conducted at lower strain or loading rates that are more typical of geotechnical testing.

This Gompertz model fit the measured data points in the compression characteristic closely, with mean $R^2$ values greater than 0.99. The estimated *Cc* values, among others (the Gompertz model parameters and the respective confidence intervals) were evaluated. This approach was also adopted by Baumgartl and Köck, 2004;to model soil compression. Furthermore, studies of the soil compression characteristics for non-agricultural purposes, such as civil engineering, have also been reported (Arvidsson and Keller, 2004; Keller and Lamandé, 2010; Kurnaz et al., 2016).

Tables 2a and 2b summarize the *Cc* values for the various soil sample compositions. The following factors, referred to equation 2, are reported: K number case; Cc = compression index; a = parameter a of Gompertz model; b = parameter b of Gompertz model; c = parameter c of Gompertz model; m = parameter m of Gompertz model; SD_a = Standard deviation of a; a_min = minimum value of a; a_max = maximum value of a; SD_b = Standard deviation of b; b_min = minimum value of b; b_max = maximum value of b; SD_c = Standard deviation of c; c_min = minimum value of c; c_max = maximum value of c; SD_m = Standard deviation of m; m_min = minimum value of m; m_max = maximum value of m.

Figure 3 shows the raw data of the S01_U5 soil compression test, the Gompertz model fit and the maximum slope line.

The estimates of *Cc*, as reported in Tables 2a and 2b, were generally greater for soils with a high moisture

**Table 2a**. Estimated Cc compression index for the soil samples considered S1-S12

| k | Soil sample | Cc | a | b | c | m | SD_a | a_min | a_max | SD_b | b_min | b_max | SD_c | c_min | c_max | SD_m | m_min | m_max |
|---|---|---|---|---|---|---|---|---|---|---|---|---|---|---|---|---|---|---|
| 1 | S01U0 | **0.039** | 0.470 | 0.850 | 0.124 | 4.495 | 0.007 | 0.450 | 0.489 | 0.061 | 0.680 | 1.019 | 0.009 | 0.099 | 0.149 | 0.101 | 4.216 | 4.774 |
| 2 | S01U5 | **0.113** | 0.591 | 1.029 | 0.298 | 4.289 | 0.006 | 0.573 | 0.609 | 0.040 | 0.917 | 1.141 | 0.009 | 0.272 | 0.324 | 0.033 | 4.197 | 4.381 |
| 3 | S01U10 | **0.195** | 0.543 | 1.082 | 0.489 | 4.245 | 0.005 | 0.528 | 0.557 | 0.023 | 1.019 | 1.146 | 0.008 | 0.468 | 0.511 | 0.016 | 4.202 | 4.289 |
| 4 | S02U0 | **0.039** | 0.502 | 0.906 | 0.118 | 4.488 | 0.004 | 0.490 | 0.515 | 0.044 | 0.783 | 1.029 | 0.006 | 0.102 | 0.133 | 0.065 | 4.308 | 4.669 |
| 5 | S02U5 | **0.111** | 0.606 | 0.980 | 0.308 | 4.296 | 0.006 | 0.588 | 0.624 | 0.036 | 0.879 | 1.081 | 0.009 | 0.282 | 0.334 | 0.033 | 4.203 | 4.388 |
| 6 | S02U10 | **0.184** | 0.574 | 1.059 | 0.473 | 4.231 | 0.006 | 0.556 | 0.591 | 0.029 | 0.979 | 1.139 | 0.010 | 0.446 | 0.500 | 0.020 | 4.175 | 4.287 |
| 7 | S03U0 | **0.042** | 0.545 | 0.864 | 0.133 | 4.262 | 0.008 | 0.523 | 0.567 | 0.092 | 0.609 | 1.118 | 0.012 | 0.100 | 0.167 | 0.101 | 3.982 | 4.543 |
| 8 | S03U5 | **0.106** | 0.571 | 1.132 | 0.256 | 5.024 | 0.095 | 0.306 | 0.837 | 0.240 | 0.465 | 1.798 | 0.101 | -0.026 | 0.537 | 0.524 | 3.567 | 6.481 |
| 9 | S03U10 | **0.180** | 0.556 | 0.999 | 0.354 | 5.024 | 0.097 | 0.287 | 0.825 | 0.165 | 0.539 | 1.459 | 0.104 | 0.065 | 0.643 | 0.432 | 3.823 | 6.225 |
| 10 | S04U0 | **0.039** | 0.591 | 0.888 | 0.120 | 4.497 | 0.005 | 0.578 | 0.605 | 0.046 | 0.761 | 1.016 | 0.006 | 0.102 | 0.137 | 0.070 | 4.302 | 4.692 |
| 11 | S04U5 | **0.108** | 0.630 | 0.972 | 0.303 | 4.432 | 0.009 | 0.606 | 0.655 | 0.041 | 0.858 | 1.086 | 0.012 | 0.270 | 0.335 | 0.048 | 4.299 | 4.565 |
| 12 | S04U10 | **0.179** | 0.624 | 1.012 | 0.480 | 4.130 | 0.009 | 0.598 | 0.649 | 0.045 | 0.887 | 1.137 | 0.015 | 0.437 | 0.523 | 0.029 | 4.049 | 4.211 |
| 13 | S05U0 | **0.039** | 0.606 | 0.932 | 0.114 | 4.463 | 0.004 | 0.594 | 0.617 | 0.045 | 0.808 | 1.056 | 0.005 | 0.100 | 0.129 | 0.059 | 4.298 | 4.628 |
| 14 | S05U5 | **0.106** | 0.662 | 0.974 | 0.296 | 4.393 | 0.010 | 0.635 | 0.690 | 0.050 | 0.836 | 1.112 | 0.013 | 0.258 | 0.333 | 0.054 | 4.242 | 4.543 |
| 15 | S05U10 | **0.191** | 0.618 | 1.026 | 0.507 | 4.269 | 0.006 | 0.603 | 0.634 | 0.022 | 0.965 | 1.086 | 0.008 | 0.484 | 0.531 | 0.017 | 4.221 | 4.317 |
| 16 | S06U0 | **0.039** | 0.612 | 0.925 | 0.116 | 4.487 | 0.004 | 0.600 | 0.624 | 0.045 | 0.801 | 1.050 | 0.006 | 0.100 | 0.131 | 0.063 | 4.312 | 4.662 |
| 17 | S06U5 | **0.108** | 0.690 | 1.033 | 0.284 | 4.395 | 0.008 | 0.667 | 0.713 | 0.046 | 0.905 | 1.161 | 0.011 | 0.254 | 0.315 | 0.045 | 4.270 | 4.521 |
| 18 | S06U10 | **0.178** | 0.658 | 1.087 | 0.445 | 4.277 | 0.006 | 0.641 | 0.675 | 0.029 | 1.006 | 1.167 | 0.009 | 0.420 | 0.471 | 0.021 | 4.219 | 4.335 |
| 19 | S07U0 | **0.075** | 0.818 | 1.029 | 0.198 | 4.420 | 0.008 | 0.796 | 0.841 | 0.062 | 0.857 | 1.201 | 0.011 | 0.168 | 0.227 | 0.064 | 4.242 | 4.598 |
| 20 | S07U5 | **0.141** | 0.452 | 0.987 | 0.387 | 4.792 | 0.025 | 0.382 | 0.522 | 0.054 | 0.836 | 1.138 | 0.029 | 0.307 | 0.467 | 0.107 | 4.496 | 5.089 |
| 21 | S07U10 | **0.272** | 0.330 | 1.145 | 0.646 | 4.925 | 0.086 | 0.092 | 0.568 | 0.100 | 0.868 | 1.422 | 0.092 | 0.390 | 0.902 | 0.187 | 4.407 | 5.444 |
| 22 | S08U0 | **0.075** | 0.844 | 0.988 | 0.207 | 4.515 | 0.009 | 0.818 | 0.869 | 0.056 | 0.833 | 1.143 | 0.012 | 0.175 | 0.240 | 0.073 | 4.313 | 4.717 |
| 23 | S08U5 | **0.136** | 0.492 | 1.012 | 0.365 | 4.723 | 0.021 | 0.434 | 0.549 | 0.053 | 0.865 | 1.159 | 0.024 | 0.299 | 0.431 | 0.091 | 4.471 | 4.974 |
| 24 | S08U10 | **0.279** | 0.330 | 1.106 | 0.686 | 5.022 | 0.060 | 0.164 | 0.497 | 0.056 | 0.951 | 1.260 | 0.064 | 0.509 | 0.864 | 0.125 | 4.673 | 5.371 |
| 25 | S09U0 | **0.075** | 0.887 | 0.877 | 0.233 | 4.721 | 0.022 | 0.826 | 0.949 | 0.079 | 0.656 | 1.098 | 0.026 | 0.160 | 0.305 | 0.171 | 4.246 | 5.196 |
| 26 | S09U5 | **0.138** | 0.483 | 0.942 | 0.400 | 4.868 | 0.031 | 0.397 | 0.570 | 0.056 | 0.785 | 1.098 | 0.035 | 0.303 | 0.496 | 0.132 | 4.502 | 5.235 |
| 27 | S09U10 | **0.283** | 0.355 | 1.115 | 0.690 | 5.024 | 0.074 | 0.148 | 0.561 | 0.069 | 0.925 | 1.306 | 0.079 | 0.471 | 0.909 | 0.153 | 4.599 | 5.449 |
| 28 | S10U0 | **0.075** | 0.901 | 0.867 | 0.236 | 4.640 | 0.017 | 0.854 | 0.948 | 0.067 | 0.681 | 1.052 | 0.021 | 0.178 | 0.294 | 0.131 | 4.275 | 5.004 |
| 29 | S10U5 | **0.138** | 0.536 | 0.990 | 0.378 | 4.766 | 0.024 | 0.469 | 0.604 | 0.056 | 0.836 | 1.145 | 0.028 | 0.300 | 0.455 | 0.105 | 4.474 | 5.059 |
| 30 | S10U10 | **0.287** | 0.373 | 1.124 | 0.694 | 5.024 | 0.098 | 0.100 | 0.647 | 0.091 | 0.872 | 1.376 | 0.105 | 0.403 | 0.984 | 0.200 | 4.467 | 5.581 |
| 31 | S11U0 | **0.075** | 0.937 | 0.938 | 0.217 | 4.623 | 0.014 | 0.898 | 0.976 | 0.066 | 0.755 | 1.121 | 0.017 | 0.169 | 0.264 | 0.111 | 4.315 | 4.930 |
| 32 | S11U5 | **0.142** | 0.542 | 0.984 | 0.391 | 4.853 | 0.027 | 0.467 | 0.617 | 0.052 | 0.839 | 1.129 | 0.030 | 0.308 | 0.474 | 0.112 | 4.542 | 5.164 |
| 33 | S11U10 | **0.278** | 0.409 | 1.099 | 0.688 | 5.024 | 0.043 | 0.290 | 0.528 | 0.039 | 0.989 | 1.209 | 0.046 | 0.561 | 0.815 | 0.090 | 4.774 | 5.274 |
| 34 | S12U0 | **0.077** | 0.686 | 0.947 | 0.220 | 4.701 | 0.016 | 0.643 | 0.729 | 0.064 | 0.768 | 1.126 | 0.018 | 0.170 | 0.271 | 0.119 | 4.369 | 5.033 |
| 35 | S12U5 | **0.136** | 0.448 | 0.993 | 0.372 | 4.768 | 0.021 | 0.389 | 0.507 | 0.049 | 0.856 | 1.129 | 0.024 | 0.305 | 0.439 | 0.093 | 4.511 | 5.025 |
| 36 | S12U10 | **0.262** | 0.330 | 1.130 | 0.631 | 4.914 | 0.058 | 0.170 | 0.490 | 0.069 | 0.938 | 1.323 | 0.062 | 0.458 | 0.804 | 0.130 | 4.551 | 5.276 |

*SD = standard deviation – Cc =compressionindex*

**Table 2b.** Estimated Cc compression indexfor the soil samples considered S13-S24

| k | Soil sample | Cc | a | b | c | m | SD_a | a_min | a_max | SD_b | b_min | b_max | SD_c | c_min | c_max | SD_m | m_min | m_max |
|---|---|---|---|---|---|---|---|---|---|---|---|---|---|---|---|---|---|---|
| 37 | S13U0 | **0.076** | 0.803 | 1.040 | 0.197 | 4.500 | 0.009 | 0.777 | 0.829 | 0.064 | 0.862 | 1.218 | 0.012 | 0.164 | 0.230 | 0.074 | 4.294 | 4.706 |
| 38 | S13U5 | **0.135** | 0.480 | 0.992 | 0.369 | 4.696 | 0.020 | 0.423 | 0.536 | 0.053 | 0.846 | 1.139 | 0.024 | 0.303 | 0.435 | 0.090 | 4.446 | 4.946 |
| 39 | S13U10 | **0.262** | 0.330 | 1.075 | 0.663 | 5.024 | 0.056 | 0.174 | 0.486 | 0.053 | 0.928 | 1.222 | 0.060 | 0.497 | 0.829 | 0.125 | 4.678 | 5.370 |
| 40 | S14U0 | **0.077** | 0.815 | 0.965 | 0.216 | 4.582 | 0.010 | 0.788 | 0.843 | 0.051 | 0.823 | 1.106 | 0.012 | 0.182 | 0.250 | 0.077 | 4.368 | 4.795 |
| 41 | S14U5 | **0.137** | 0.508 | 1.027 | 0.363 | 4.606 | 0.013 | 0.472 | 0.545 | 0.041 | 0.913 | 1.141 | 0.016 | 0.319 | 0.407 | 0.057 | 4.446 | 4.766 |
| 42 | S14U10 | **0.296** | 0.330 | 1.171 | 0.687 | 4.999 | 0.114 | 0.012 | 0.648 | 0.113 | 0.857 | 1.486 | 0.121 | 0.349 | 1.024 | 0.227 | 4.368 | 5.630 |
| 43 | S15U0 | **0.079** | 0.840 | 0.943 | 0.226 | 4.745 | 0.018 | 0.789 | 0.890 | 0.068 | 0.753 | 1.132 | 0.021 | 0.168 | 0.284 | 0.136 | 4.368 | 5.121 |
| 44 | S15U5 | **0.138** | 0.486 | 0.954 | 0.394 | 4.845 | 0.026 | 0.414 | 0.558 | 0.050 | 0.816 | 1.092 | 0.029 | 0.313 | 0.475 | 0.110 | 4.538 | 5.152 |
| 45 | S15U10 | **0.306** | 0.341 | 1.185 | 0.702 | 5.024 | 0.140 | -0.049 | 0.730 | 0.131 | 0.821 | 1.550 | 0.148 | 0.291 | 1.113 | 0.268 | 4.280 | 5.768 |
| 46 | S16U0 | **0.049** | 0.683 | 0.895 | 0.149 | 4.887 | 0.019 | 0.631 | 0.734 | 0.085 | 0.658 | 1.132 | 0.021 | 0.091 | 0.207 | 0.220 | 4.275 | 5.499 |
| 47 | S16U5 | **0.074** | 0.722 | 0.964 | 0.209 | 4.240 | 0.008 | 0.700 | 0.743 | 0.068 | 0.776 | 1.152 | 0.012 | 0.176 | 0.241 | 0.058 | 4.079 | 4.401 |
| 48 | S16U10 | **0.215** | 0.409 | 0.987 | 0.591 | 5.024 | 0.057 | 0.252 | 0.566 | 0.058 | 0.826 | 1.147 | 0.061 | 0.422 | 0.760 | 0.153 | 4.598 | 5.450 |
| 49 | S17U0 | **0.049** | 0.700 | 0.775 | 0.173 | 5.024 | 0.029 | 0.619 | 0.782 | 0.093 | 0.517 | 1.034 | 0.033 | 0.082 | 0.264 | 0.341 | 4.076 | 5.971 |
| 50 | S17U5 | **0.073** | 0.735 | 0.959 | 0.208 | 4.383 | 0.012 | 0.702 | 0.767 | 0.082 | 0.732 | 1.185 | 0.016 | 0.164 | 0.252 | 0.091 | 4.131 | 4.635 |
| 51 | S17U10 | **0.208** | 0.446 | 0.972 | 0.581 | 4.902 | 0.028 | 0.368 | 0.523 | 0.034 | 0.878 | 1.066 | 0.031 | 0.495 | 0.666 | 0.079 | 4.683 | 5.121 |
| 52 | S18U0 | **0.048** | 0.736 | 0.875 | 0.149 | 4.821 | 0.019 | 0.683 | 0.789 | 0.094 | 0.613 | 1.137 | 0.022 | 0.088 | 0.210 | 0.232 | 4.178 | 5.465 |
| 53 | S18U5 | **0.076** | 0.769 | 1.007 | 0.205 | 4.332 | 0.006 | 0.751 | 0.786 | 0.052 | 0.862 | 1.152 | 0.009 | 0.181 | 0.230 | 0.048 | 4.198 | 4.467 |
| 54 | S18U10 | **0.208** | 0.441 | 0.951 | 0.594 | 5.023 | 0.037 | 0.338 | 0.544 | 0.037 | 0.848 | 1.054 | 0.040 | 0.483 | 0.706 | 0.103 | 4.736 | 5.311 |
| 55 | S19U0 | **0.049** | 0.730 | 0.927 | 0.143 | 4.767 | 0.024 | 0.662 | 0.797 | 0.139 | 0.540 | 1.314 | 0.028 | 0.065 | 0.221 | 0.293 | 3.954 | 5.580 |
| 56 | S19U5 | **0.075** | 0.739 | 1.066 | 0.193 | 4.296 | 0.008 | 0.716 | 0.762 | 0.084 | 0.832 | 1.299 | 0.012 | 0.159 | 0.226 | 0.065 | 4.115 | 4.476 |
| 57 | S19U10 | **0.213** | 0.399 | 0.996 | 0.580 | 5.024 | 0.053 | 0.251 | 0.546 | 0.055 | 0.843 | 1.150 | 0.057 | 0.422 | 0.739 | 0.145 | 4.621 | 5.426 |
| 58 | S20U0 | **0.048** | 0.775 | 0.901 | 0.144 | 4.776 | 0.017 | 0.727 | 0.823 | 0.095 | 0.637 | 1.165 | 0.020 | 0.089 | 0.200 | 0.211 | 4.190 | 5.362 |
| 59 | S20U5 | **0.073** | 0.755 | 0.925 | 0.215 | 4.303 | 0.010 | 0.726 | 0.784 | 0.076 | 0.713 | 1.136 | 0.015 | 0.174 | 0.257 | 0.079 | 4.084 | 4.523 |
| 60 | S20U10 | **0.235** | 0.366 | 1.026 | 0.622 | 5.024 | 0.075 | 0.158 | 0.574 | 0.074 | 0.821 | 1.231 | 0.080 | 0.399 | 0.845 | 0.186 | 4.507 | 5.540 |
| 61 | S21U0 | **0.047** | 0.810 | 0.961 | 0.133 | 4.633 | 0.013 | 0.774 | 0.846 | 0.098 | 0.687 | 1.234 | 0.015 | 0.090 | 0.176 | 0.162 | 4.183 | 5.082 |
| 62 | S21U5 | **0.074** | 0.787 | 0.969 | 0.207 | 4.322 | 0.009 | 0.762 | 0.812 | 0.072 | 0.769 | 1.169 | 0.013 | 0.171 | 0.243 | 0.071 | 4.126 | 4.518 |
| 63 | S21U10 | **0.249** | 0.375 | 1.035 | 0.653 | 5.024 | 0.053 | 0.228 | 0.522 | 0.050 | 0.896 | 1.174 | 0.057 | 0.496 | 0.811 | 0.124 | 4.679 | 5.368 |
| 64 | S22U0 | **0.049** | 0.737 | 0.774 | 0.173 | 5.024 | 0.032 | 0.650 | 0.825 | 0.100 | 0.495 | 1.052 | 0.035 | 0.074 | 0.271 | 0.369 | 4.000 | 6.048 |
| 65 | S22U5 | **0.076** | 0.696 | 0.853 | 0.241 | 4.568 | 0.016 | 0.651 | 0.741 | 0.068 | 0.665 | 1.041 | 0.020 | 0.184 | 0.298 | 0.123 | 4.226 | 4.911 |
| 66 | S22U10 | **0.165** | 0.508 | 1.075 | 0.418 | 5.024 | 0.241 | -0.160 | 1.177 | 0.361 | 0.072 | 2.079 | 0.257 | -0.295 | 1.131 | 0.849 | 2.664 | 7.383 |
| 67 | S23U0 | **0.049** | 0.762 | 0.775 | 0.173 | 5.024 | 0.032 | 0.672 | 0.852 | 0.102 | 0.491 | 1.060 | 0.036 | 0.072 | 0.273 | 0.375 | 3.982 | 6.066 |
| 68 | S23U5 | **0.073** | 0.745 | 0.927 | 0.215 | 4.299 | 0.010 | 0.717 | 0.774 | 0.076 | 0.715 | 1.139 | 0.015 | 0.173 | 0.256 | 0.078 | 4.081 | 4.516 |
| 69 | S23U10 | **0.218** | 0.409 | 1.014 | 0.585 | 5.024 | 0.052 | 0.265 | 0.553 | 0.054 | 0.863 | 1.164 | 0.056 | 0.430 | 0.739 | 0.138 | 4.639 | 5.408 |
| 70 | S24U0 | **0.049** | 0.792 | 0.775 | 0.173 | 5.024 | 0.032 | 0.702 | 0.882 | 0.102 | 0.491 | 1.060 | 0.036 | 0.072 | 0.273 | 0.375 | 3.982 | 6.066 |
| 71 | S24U5 | **0.075** | 0.780 | 1.027 | 0.199 | 4.334 | 0.008 | 0.758 | 0.801 | 0.068 | 0.838 | 1.217 | 0.011 | 0.169 | 0.230 | 0.061 | 4.165 | 4.504 |
| 72 | S24U10 | **0.216** | 0.446 | 1.003 | 0.586 | 5.024 | 0.050 | 0.308 | 0.584 | 0.051 | 0.860 | 1.145 | 0.053 | 0.438 | 0.734 | 0.133 | 4.653 | 5.395 |

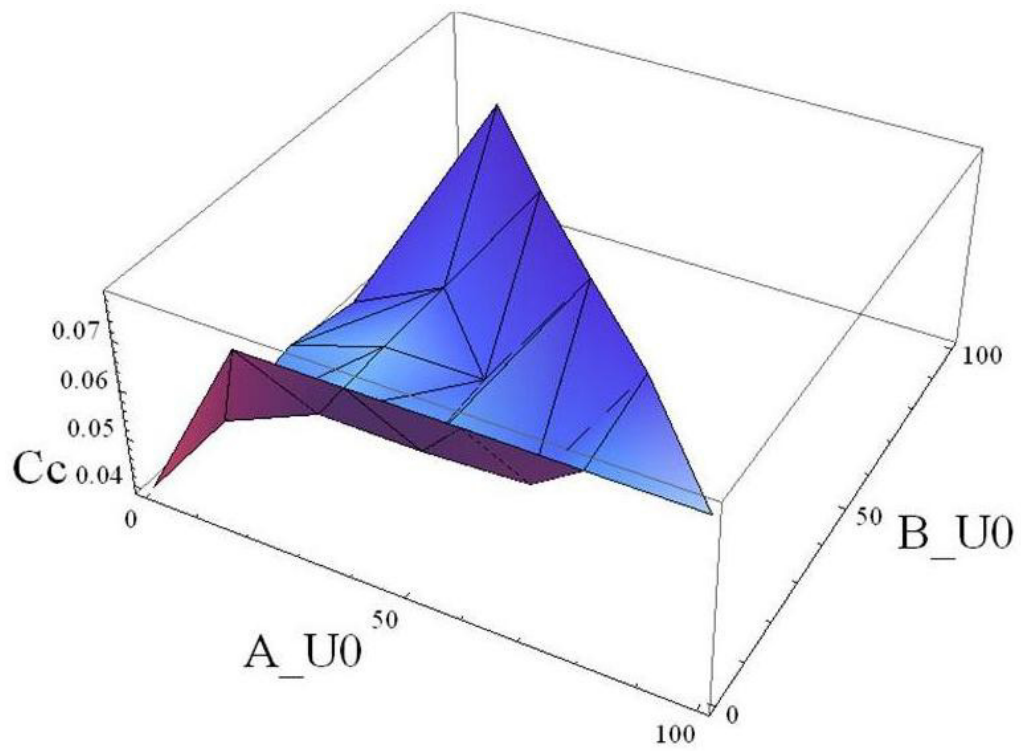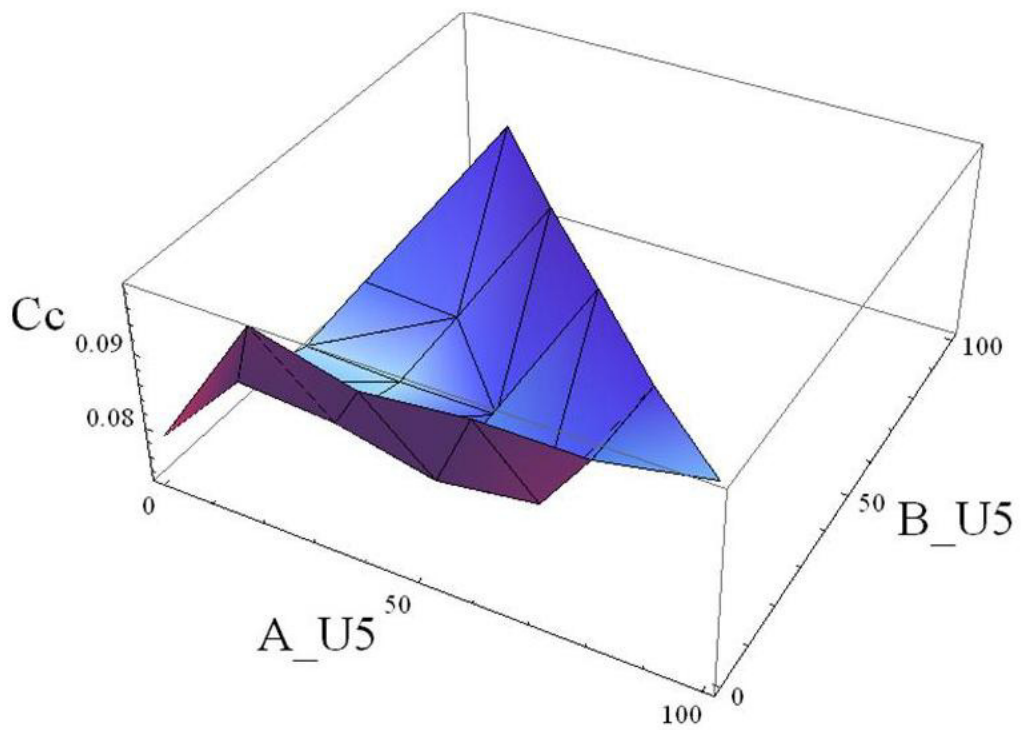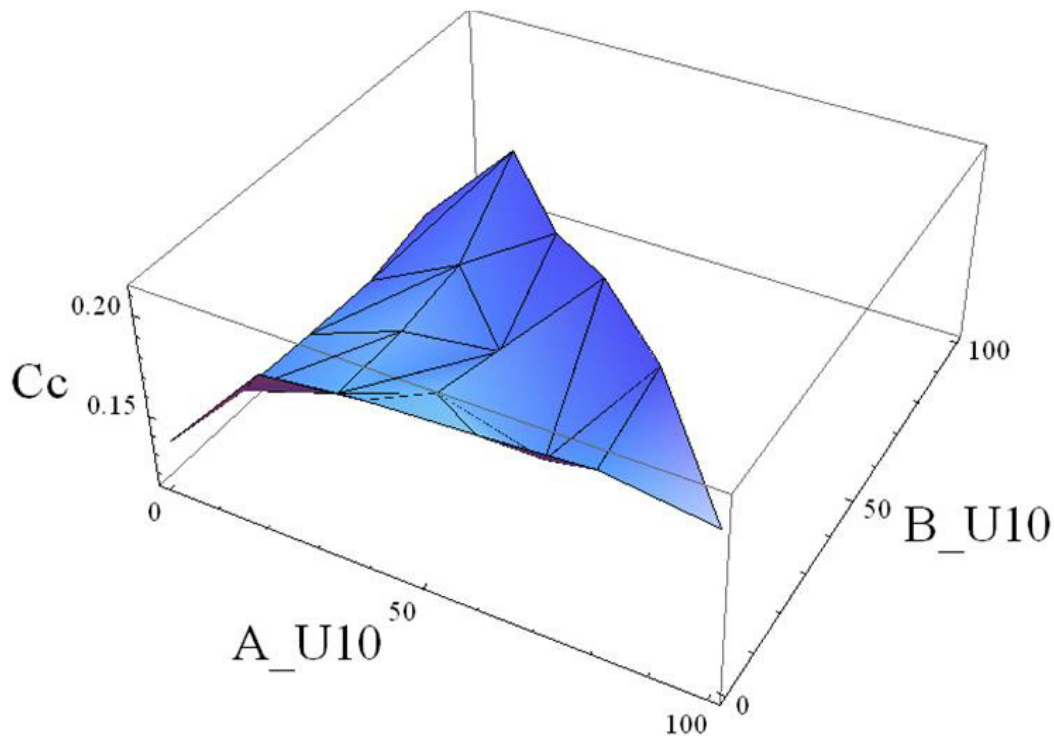*SD = standard deviation – Cc =compression index*

**Figure 4a**



**Figure 4b**

**Figure 4c**

**Figure 4 (a,b,c)** 3D diagrams of the obtained values for different granulometry:
(a) A, B with moisture U= 0 %
(b)A, B with moisture U= 5 %
(c) A, B with moisture U= 10%

content. Similar findings were reported by Imhoff*et al.*, 2004.

Figures 4(a,b,c) show the 3D diagram of the function Cc=f(A,B) at u=0, 5, 10%, respectively. These diagrams are the graphical representation of the Cc values shown in Tables 2a and 2b. Using these diagrams the gradient changes of the considered Cc can be evaluated. With the values of U = 0% and U = 5%, the trend of the gradient of the Cc function is similar, while for U = 10%, the Cc gradient changes considerably.

The diagrams presented here are in agreement with the findings obtained by previous studies (Fredlund and Rahardjo, 1993; Batey, 2009; Zolotarevskaya, 2011). Furthermore, in these diagrams, the Cc gradient values, as a function of the granulometry values, decrease when the moisture contents increase.

Examining tables 2a and 2b and diagrams 4 (a, b, c) show that:

for U=0%, Cc max is obtained for soil composition S15 (A=80%; B=20%; C=0%);

for U=5%, Cc max is obtained for soil composition

S11(A=100%; B=0%; C=0%); and

for U=10%, Cc max is obtained for soil composition S15(A=80%; B=20%; C=0%).

**DISCUSSION**

It is diffuse the way to fit compression diagram to the compression parameter in order to evaluate the coordinates of maximum curvature analytically. Data results describing the soil compression parameters have been fitted by numerous authors, in different way: polynomial (Arvidsson and Keller, 2004), sigmoidal (Baumgartl and Köck, 2004), etc.

However, all the methods used up to now have advantages and disadvantages; each method has an approximation grade to describe the value of Cc. Further, a number of other possibilities based on the compression characteristic can be also used to define that point where reversible elastic failure becomes irreversible plastic deformation. These include the point of maximum

curvature itself and the intercept of the linear virgin curve with a horizontal line drawn at zero stress (Arvidsson and Keller, 2004) or the intercept with a tangent at low stress (Fredlundand, Rahardjo, 1993; Chaney et al., 2001; Vallejos, 2008; Gregory et al., 2006).

However, in this paper, we pointed acomparison between the Cc values computed by linear interpolation (LI), using the first two points of the diagram, and by the Gompertz Model (GM) computed in this research. The values obtained with the GM method were always lower than the values obtained with the LI method. Furthermore, the data revealed the following:

-the Cc increases with increasing the moisture content;

-for sandy soils formed with constant Agranulometry, and granulometry B and C variables (%), increasing B%, the Cc value changed very little;

-for sandy soils formed with constant B granulometry, and granulometryA and C variables (%), increasing A%, the Cc value changed robustly;

-for sandy soils formed with constant C granulometry, and granulometryA and B variables (%), increasing A%, the Cc value changed robustly.

Therefore, increases in the percent of big granulometry (A) in the sandy soil composition resulted in meaningful changes to the Cc value.

## CONCLUSIONS

The obtained data show that at the same moisture value but different granulometry, the slopes of the curves depend on the granulometry value. Furthermore, the effects due to granulometry decrease when the moisture increases. The considered soil and soil-tool interaction can be characterized using an easily determined soil model. The data presented here agree with the well regarded theories about soil compression and confirmed the validity of the experimental tests performed. Subsequently, the compression index *Cc* was evaluated for the soil samples using the asymmetrical S-shaped Gompertz model. The influence on compression phenomenon due to the granulometry composition decreases when the moisture content increases.

This study discover the influence of the soil granulometry composition and moisture content on the compression index Cc by mean a systematic study of 24 soil typologies representative of almost all types of sandy soils. That can be beneficial for the evaluation of the behaviour of the considered sandy soil submitted at compression loads denoting the soil compaction capability and alterations in the Cc value when soil granulometry composition and moisture change.

**REFERENCES**

Abo-Elnor M, Hamilton R, Boyle JT (2003). 3D Dynamic analysis of soil–tool interaction using the finite element method. Journal ofTerramechanics 40: 51-62

Ansorge D, Godwin RJ(2009). An in-situ determination of virgin compression line parameters for predicting soil displacement resulting from agricultural tire passes. Journal ofTerramechanics 46: 251-258

Arvidsson J, Keller T (2004). Soil precompression stress. Soil and Tillage Research 77: 85-95

Batey T (2009). Soil compaction and soil management a review. Soil Use and Management 25: 335–345

Baumgartl T, Köck B (2004).Modeling volume change and mechanical properties with hydraulic models.*Soil Science Society of America Journal* 68: 57-65

Beylich A, Oberholzer HR, Schrader S, Höper H, Wilke BM (2010). Evaluation of soil compaction effects on soil biota and soil biological processes in soils. Soil and Tillage Research 109: 133-143

Botta G, Jorajuria D, Rosatto H, Ferrero C (2006). Light tractor traffic frequency on soil compaction in the Rolling Pampa region of Argentina. Soil and Tillage Research 86: 9-14

Botta G, Rivero D, Tourn M, Melcon F, Pozzolo O, Nardon G(2008). Soil compaction produced by tractor with radial and cross-ply tyres in two tillage regimes. Soil and Tillage Research 101: 44–51

Chaney R,Demars K, Macari E, Hoyos L (2001). Mechanical behavior of an unsaturated soil under multi-axial stress states. Geotechnical Testing Journal 24: 14-22

Formato A (2005). Simplified triaxial apparatus to test agricultural soils. Soil and Tillage Research 81: 121-129

Formato A, Faugno S, Paolillo G (2005). Numerical simulation of the interaction between soil and plough mouldboard. Biosystem Engineering 93: 309-316

Formato A, Pucillo GP, Abagnale A (2013). Study of sandy soil compaction. Journal of Agricultural Science and Technology (A) 3, (5), 356-367

Fredlund DG, Rahardjo H (1993). Soil mechanics of unsaturated soils, J. Wiley and Sons IncEditor, NewYork

Gregory AS, Whalley WR, Watts CW, Bird NRA, Hallett PD, Whitmore AP (2006). Calculation of the compression index and precompression stress from soil compression test data. Soil and Tillage Research 89: 45-57

Güllü H, Canakci H, Alhashemy A (2016).Development of correlations for compression index. AfyonKocatepe University Journal of Sciences and Engineering 16: 344  355

Honda M, Ohno S, Iizuka A, Kawai K, Ohta H (2011). Theoretical evaluation of the mechanical behavior of unsaturated soils. Geotechnical and Geological Engineering29: 171-180

Imhoff S, Da Silva AP, Fallow D (2004). Susceptibility to compaction, load support capacity, and soil compressibility of Hapludox.Soil Science Society of America Journal68: 17-24

International Journal of Innovative Technology 4: 34-37.

Karmakar S, Kushwaha RL (2006). Dynamic modelling of soil–tool interaction: an overview from a fluid flow perspective. Journal ofTerramechanics 43: 411- 425

Keller T, Défossez P, Weisskopf P, Arvidsson J, Richard G(2007). Soil-Flex: A model for prediction of soil stresses and soil compaction due to agricultural field traffic including a synthesis of analytical approaches. Soil and Tillage Research, 93: 391-411

Keller T, Lamandé M (2010). Challenges in the development of analytical soil compaction models. Soil and Tillage Research 111: 54-64

Kumar JV, Dixit M, Chitra R (2015) Correlation of plasticity index and compression index of soil. International Journal of Information and Education Technology5: 263-270

Kurnaz TF, Dagdeviren U, Yildiz M, Ozkan O (2016). Prediction of compressibility parameters of the soils using artificial neural network. Springer Plus5 (1): 1801

Mekkiyah HM, Al-Khazragie A (2015). Behavior of clay soil mixed with fine sand During consolidation. Journal of Applied Research 1: 437-443.

Mosaddeghi MR, Koolen AJ, Hajabbasi MA, Hemmat A, Keller T (2007). Suitability of pre-compression stress as the real critical stress of unsaturated agricultural soils. BiosystemEngineering 98: 90-101

Peruzzi A, Raffaelli M, Ginanni M, Fontanelli M (2008). The rolling harrow: A new operative machine for physical weed control. [In review]. In: Book: advances in soil and tillage research. Transworld research network Editor 37/661 (2), Fort P.O., Trivandrum - 695023, Kerala, India 1:159-172.

Singh SNA (2012). Soil compression index prediction model for fine grained soils.

Tekeste MZ, Tollner EW, Raper RL, Way TR, Johnson CE (2009). Non-linear finite element analysis of cone penetration in layered sandy loam soil - Considering pre-compression stress state. Journal ofTerramechanics 46: 229-239

Tiwari BT, Ajmera B (2012). New Correlation Equations for Compression Index of Remolded Clays.Journal of Geotechnical and Geo-environmental Engineering 138: 757-762

Vallejos J (2008). Hydrostatic compression model for sandy soils. Canadian Geotechnical Journal 45: 1169-1179

Zolotarevskaya D(2011). Mathematical simulation and calculation of the soil compaction under dynamic loads. ESA Soil Science, 4: 407-416